Proceedings of the Thirty-fourth (2024) International Ocean and Polar Engineering Conference **www.isope.org**
Rhodes, Greece, June 16–21, 2024

ISBN 978-1-880653-78-4; ISSN 1098-6189

On Modeling the Coastal Floods and Assessing the Impacts on Inundated Urban Areas of Miami (FL, USA)

Christos V. Makris, Yannis S. Androulidakis, Zisis C. Mallios
Department of Civil Engineering, Faculty of Engineering, Aristotle University of Thessaloniki
Thessaloniki, Central Macedonia, Greece

Villy H. Kourafalou
Rosenstiel School of Marine Atmospheric and Earth Science, University of Miami
Miami, Florida, USA

ABSTRACT

In this paper, we present recent developments of CoastFLOOD model for the high-resolution simulation of coastal inundation induced by the Total Water Level along the shoreline, considering the 30-year extreme Sea Level Elevation due to storm surge, intensified by high astronomical tides and wave-induced set-up. The scope of the study is to assess the interannual spatial variability of impacts from coastal inundation due to seawater flooding over characteristic urban areas of Miami. In conclusion, we evaluate the flood exposure at building-level around properties located on the Biscayne Bay coasts and Miami Beach.

KEY WORDS: Coastal flooding; sea level elevation; coastal hazard; inundation maps; impact assessment; exposure; Miami.

INTRODUCTION

The variability of nearshore Sea Level Elevation (SLE) is a key indicator of global-scale climatic changes with significant impacts on low-lying coastal areas (Williams & Gutierrez, 2009). As such, South Florida (USA) is one of the most vulnerable regions worldwide to episodic coastal inundation due to extreme sea levels caused by tropical storms and hurricanes (Jones et al., 2019). Specifically, the natural and urban coastal environment in and around Miami is a hotspot for climate-related adverse effects (Palm & Bolsen, 2020). Severe storm surge has impacted the study region's low-land littoral areas in the past, by causing inundation over coastal floodplains and exposed urban settings (Ghorbanzadeh et al., 2021). Especially when storm surge coincides with high tides (storm tides), enhanced further by the recent mean Sea Level Rise (SLR), it can cause land loss, coastal erosion, damages to onshore infrastructure and properties, human casualties, degradation of coastal ecosystems, etc. (Genovese et al., 2011).

In this paper, we present recent developments of a numerical modeling system (Makris et al., 2023) for coastal inundation induced by the Total Water Level (TWL) along the shoreline, i.e., extreme SLE due to storm surge, intensified by high astronomical tides and SLR (Androulidakis et al., 2023a). The model was initially set up for the natural environment and small urban settings of the Mediterranean Sea's coasts (e.g., Androulidakis et al., 2023b; Skoulikaris et al., 2021) and it is hereby expanded to fit the needs for our investigation in the study region of Miami-Dade County (MDC) metropolitan area.

The scope of the study is to evaluate the interannual spatial variability of impacts from coastal inundation due to seawater flooding over a characteristic part of Miami's urban region with important residential areas. The study period refers to a recent 30-year period from 1994 to 2023. We aspire to identify in high detail all the significant environmental and socioeconomic implications that are recognized as crucial factors for the sustainability of coastal environments (Kourafalou et al., 2024). In this work, we also validate an updated version of the CoastFLOOD model (Makris et al., 2022; 2023) for littoral inundation and apply it in very high resolution (dx = 1–2 m) throughout the densely populated urban area around Biscayne Bay, including the more exposed Miami Beach. We further investigate the long-term variability and trends of measured TWL by tide-gauge records and the respective behavior of coastal inundation patterns over low-land littoral areas.

The main motivation of the study is to contribute to a better understanding of climatic impacts along the coastal areas exposed to compound flooding (Sun et al., 2024), by examining the effects of increasing sea level trends of coastal TWL on littoral inundation patterns. New characteristic metrics of exposure to flood impacts at building- and property-level are further introduced (Iliadis et al., 2023; Paulik et al., 2021) and post-processed with GIS tools for portrayal by high-resolution maps (Darlington et al., 2024). These outputs support our ongoing research about the implications of coastal flooding due to storm tides on Miami's public plot holdings and individual properties (Chao et al., 2021), by identifying their damages and relevant risk, according to the needs of local stakeholders and real-estate players

(Katirtzidou et al., 2023), which may drive changes to their prices and insurance fees (Conte & Kelly, 2018).

CASE STUDY MODEL AND DATA

Case Study Area

The coastal area of MDC in the southeastern part of Florida (USA) has been characterized as the most exposed county of the state to storm surge flooding (Chao et al., 2021). Events of extended coastal inundation are usually induced by hurricanes and tropical cyclones especially when they coincide with King Tide events. The porous geological substrate of the broader study region that permits the percolating flow of seawater to inland low-lying areas can further enhance littoral flooding of southern MDC limiting the protective effects of coastal seawalls and vegetated sand dunes.

The selection of the case study site was mainly defined by the versatile demographics and land uses, the dense population and urban intensity, the property values *in tandem* with the structural typology at building-level, and finally the computational efficiency of flood model simulations. Therefore, the study area comprises the coastal zone of southern Biscayne Bay and the mid-to-south stretch of Miami Beach on the Atlantic Ocean's shores (Fig. 1), pertaining both naturally protected and more exposed urbanized shores of the eastern Florida seaboard, several insular barriers, and the Port of Miami on Dodge Island.

Fig. 1 portrays the land elevation map of the study area on a rectangular grid of dx = 2 m spatial resolution, interpolated from a 3–6 ft resolution Digital Terrain Model (DTM), based on the US Geological Survey (USGS) Digital Surface Model (DSM) that includes natural and human-made features on the earth's surface (e.g., vegetation, trees, buildings, and other artifacts).

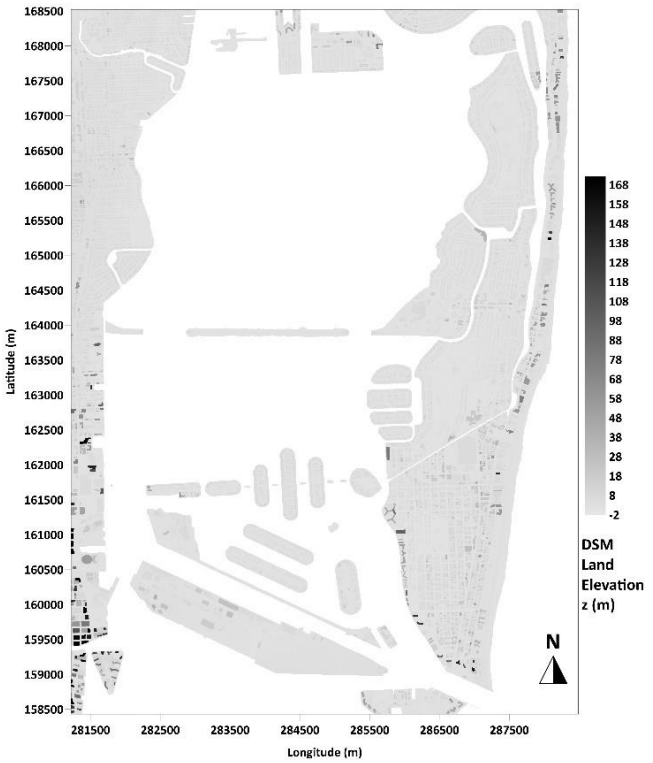

Fig. 1. Map of the Miami study area's land elevation z (m) 2 m resolution topography from measured null SLE, based on the North American Vertical Datum 1988 (NAVD-88) and NOAA's DSM.

Regarding the relevant Land Use – Land Cover (LU–LC) data in the study area, we used the codes of the USGS National Land Cover Database (NLCD) produced in association with the Multi-Resolution Land Characteristics (MRLC) consortium. The products refer to conterminous US LC at a 30 m spatial resolution with a 16–class legend, based on a modified Anderson Level II classification system, including information about recent LC changes, forest disturbance, forest tree cover, and crucial for our model urban imperviousness data (i.e., classified by types of roads, wind tower sites, building locations, built open space terrains, schools, parks, pavements, utility–infrastructure and energy production sites, etc.). We have created a 2–D LU–LC map of the Miami study area (not shown for brevity) detailly discretized per urban element, natural and human-made feature, correlated to 61 LU codes/labels (https://gis-mdc.opendata.arcgis.com/datasets/MDC::property-boundary-view/), pertaining anything from industrial facilities to bare ground and inland water bodies (https://gisweb.miamidade.gov/landinformation/). The LU–LC map was superimposed over the CoastFLOOD model's grid to assign the bottom friction data based on ground roughness by soil and built terrain type. Fig. 2 presents a map of the associated values for the Manning coefficient, n, for terrain bottom roughness based on NLCD LU–LC data for the study area. Thus, the LU–LC product has been downscaled to a 2 m spatial resolution bottom friction output, based on a 43–class grading that pertains cases for the smoothest and flattest floodplain (e.g., n=0.001 for open inland water bodies) up to the roughest terrain (e.g., n=0.4 for very dense small forest trees and thick shrubs) (Makris et al., 2023).

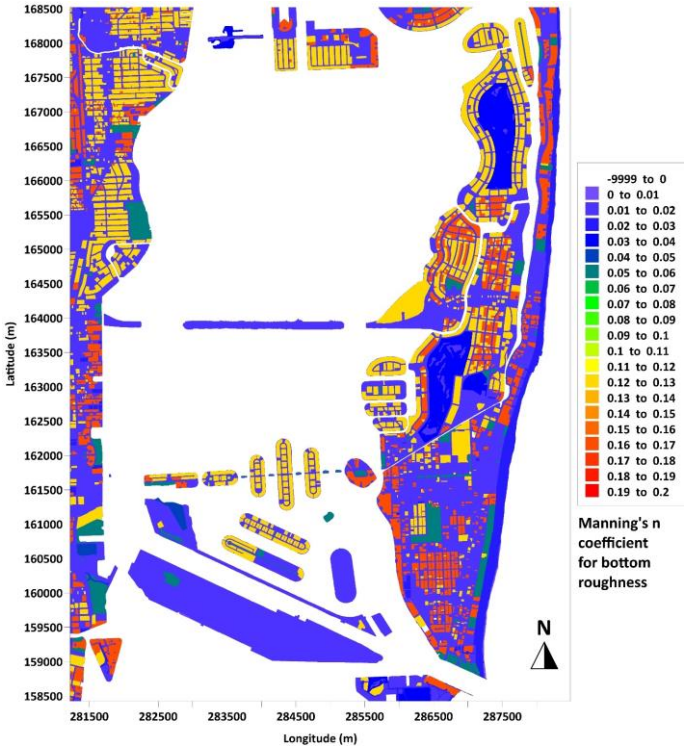

Fig. 2. Map of defined Manning n coefficient of terrain bottom roughness based on NLCD LU–LC data for the Miami study area.

Sea Level Data

Total Water Level (TWL). The used Sea Level (SL) data refer to the TWL by NOAA's tide–gauge station in Biscayne Bay's Virginia Key during the 1994-2023 period, using the same NAVD88 datum (Fig. 3a;

https://tidesandcurrents.noaa.gov/stationhome.html?id=8723214). The statistically coherent threshold of double the standard deviation (2σ) is also shown together with the trend derived by Empirical Mode Decomposition (EMD) and the annual occurrence frequency percentage of measured daily maximum SL exceeding the 2σ threshold. Increasing frequencies were computed after 2019, while negligible values occurred before 2005 in agreement with the sharp increase of the annual EMD trend during the last two decades (Fig. 3b). Moreover, the Pettit Homogeneity test (Androulidakis et al., 2023a; 2023b), derived from the annual maximum SL, showed a clear shift after 2012 (μ2-μ1 = 0.143 m). The largest recorded TWL (1.172 m) corresponds to Hurricane Irma (Category 5), that caused widespread destruction across its path, during September 2017 (Pinelli et al., 2018).

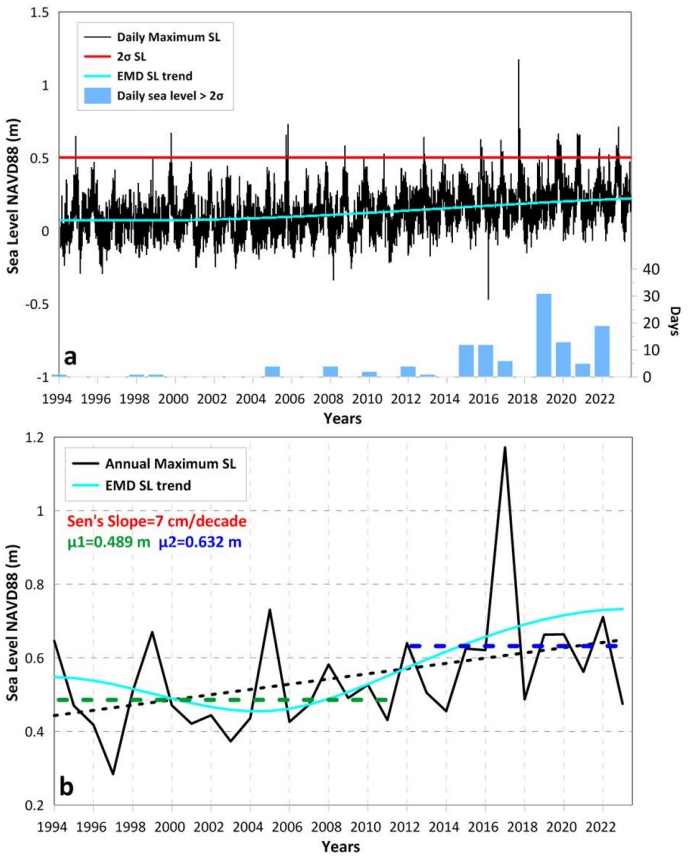

Fig. 3. (a) TWL timeseries of daily maximum Sea Level (SL; NAVD88 datum), measured at Virginia Key tide-gauge station during the 1994-2023 period. 2σ threshold (red line); EMD trend residual (blue line); annual occurrence frequency (%) of SL>2σ (bars). (b) SL annual maxima; Sen's Slope linear trend (black dashed line); EMD trend (light blue line), μ1 (green dashed line) and μ2 (blue dashed line) means.

Sea level extreme value analysis. The annual block maxima of TWL from the entire timeseries of daily SL maxima records were used to define five scenarios of extreme values for characteristic return periods (50-, 100-, 200-, 500-, and 1000-year) by a Type-III Extreme Value Analysis (EVA) following a limiting Weibull distribution fit, $W(x,\lambda,k)$, as the TWL annual maxima distribution is bounded on the upper end, using the *extRemes* package of *R*-studio (Gilleland & Katz, 2016), as follows:

$$W(x,\lambda,k) = \begin{cases} \frac{k}{\lambda}\left(\frac{x}{\lambda}\right)^{k-1} e^{-(x/\lambda)^k}, & x \geq 0 \\ 0, & x < 0 \end{cases} \quad (1)$$

where x is the random variable (i.e., *in situ* recorded TWL), k>0 is the shape parameter, and λ>0 is the scale parameter of the distribution (Galiatsatou et al., 2021). Table 1 presents 10 selected scenarios of TWL maximum percentiles and extremes for coastal flooding simulations, extracted from the recorded TWL timeseries of daily and annual maximum SL, respectively, at Virginia Key (1994-2023 period). The 30-year absolute maximum record of TWL, due to Hurricane Irma (September 2017), is estimated to exceed the 1000-year return value.

Table 1. Scenarios of TWL high percentiles (hp) and extremes (ext) for coastal flooding simulations at the MDC study area.

A/A	TWL_{hp} (m)	SLE Percentile
1	1.172	Total Maximum (100^{th})
2	0.730	99.99^{th}
3	0.664	99.95^{th}
4	0.600	99.5^{th}
5	0.510	99^{th}
A/A	**TWL_{ext} (m)**	**Return Period**
6	1.100	1000–year
7	1.055	500–year
8	1.005	200–year
9	0.963	100–year
10	0.916	50–year

Numerical Model

Coastal inundation model. The implemented coastal inundation model (CoastFLOOD, Makris et al., 2023) is a very high resolution (dx=1–2 m), raster-based, 2-D horizontal, mass balance, seawater flood simulator, which is based on the concept of reduced complexity hydraulic flow models for open floodplains and urban littorals (Neal et al., 2012). CoastFLOOD has a rather simplistic finite difference 2-D module for the continuity equation (Eq. 2) giving the local water height, h, depending on a meridional to zonal direction decomposition of the coastal inundation flow components, Q_x or Q_y (in momentum equations; x-direction example in Eq. 3), that allows the simulation of seawater propagation overland, accompanied by a dry/wet cell storage code (Bates et al., 2010; Makris et al. 2022). The flow rates at each computational cell are derived from a Manning's law approach (Fig. 2).

$$h_{i,j}^{t\prime} = h_{i,j}^{t} + dt \cdot \frac{Q_{x_{i-1/2,j}}^{t} - Q_{x_{i+1/2,j}}^{t} + Q_{y_{i,j-1/2}}^{t} - Q_{y_{i,j+1/2}}^{t}}{dx \cdot dy} \quad (2)$$

$$Q_{x_{i-1/2,j}}^{t} = \frac{h_{flow}^{t\,5/3}{}_{x_{i-1/2,j}}}{n} \cdot \left(\frac{h_{i-1,j}^{t} - h_{i,j}^{t}}{dx}\right)^{1/2} \cdot dy \quad (3)$$

where i and j are the zonal and meridional indices of the domain grid cell; h_{flow} is the flow depth between two adjacent cells, defined as the difference of the highest floodwater height minus the maximum bed elevation between two neighboring cells; dx, dy are the typical cell dimensions (spatial discretization steps); t, t' and dt are the current and next timesteps and the temporal discretization, respectively. The coastal study region can include built environments in urban areas with engineered waterfronts, ports and coastal structures, roads, highway and railway networks, and rural areas with agricultural farmlands, natural or wild vegetated fields, forests, bare-, stony-, and grass-lands, estuaries, lagoons, torrents, etc. The model is forced by the TWL scenarios derived from the 30-year measurements (Table 1).

Coastal Inundation Impact Assessment

Estimation of coastal inundation hazard. The impact of the coastal inundation hazard was estimated based on a generic Flood Cover Percentage (*FCP*, %) that was computed daily and as a cumulative 30-year index (Androulidakis et al., 2023a):

$$FCP_j = \frac{FA_j}{FA_{max}} \quad (4)$$

where FA_j is the calculated flooded area in the study region for each simulation day, *j*, of the 30-year period (only for positive TWL) based on CoastFLOOD simulation outputs, FA_{max} is the considered maximum of the exposed area to flooding based on the scenario of Hurricane Irma extreme case for the driver of coastal inundation (>1000-year return value of TWL).

Table 2. Supporting metrics for the assessment of property-level exposure to coastal inundation.

A/A	GIS attribute at property-level	Explanation of exposure metrics within property boundaries
1	FloodProb_count	Number of flooded cells
2	FloodProb_sum	Sum of flood hazard probabilities for all inundated cells
3	FloodProb_mean	Mean of flood hazard probabilities for all inundated cells
4	FloodProb_median	Median of flood hazard probabilities for all inundated cells
5	FloodProb_stdev	Standard deviation of flood hazard probabilities for all inundated cells
6	FloodProb_min	Minimum of flood hazard probabilities for all inundated cells
7	FloodProb_max	Minimum of flood hazard probabilities for all inundated cells
8	Flood Distance	Distance of the closest flooded cell to the property boundaries (=0 if plot is flooded)
9	FloodDepth_count	Number of flooded cells
10	FloodDepth_sum	Maximum of FH for all flooded cells per property
11	FloodDepth_mean	Average of FH for all flooded cells per property
12	FloodDepth_median	Median of FH for all flooded cells per property

Exposure to coastal flooding at property-level. To properly assess the coastal flood risk (set as a future goal of study) we have included preliminary quantifiable metrics in our analysis related to exposure of (plot holding) properties derived from building-level assessment by high-resolution coastal inundation modeling. This is a basic "non-structural" measure to manage seawater flooding in coastal cities and their adverse effects, as well as a prerequisite for disaster prevention and mitigation (Iliadis et al., 2023). To this end, we have estimated the *FA* percentage (%) at property-level, the vicinity of each property to the boundaries of flooded area extents, the probabilities of flood impacts and the mean encroached floodwater depth at property-level; all relevant measures of exposure are presented in Table 2. This way we can inclusively and efficiently calculate flood exposure likelihood for each building/property regarding a diverse sample of owners and stakeholders. Each property (main element-at-risk) was assessed for flood impacts using simulated *FH*s, in an effective buffer zone around its bounds, where the mean, max, high-order percentile values and other statistical measures were calculated. Herein we present the maps of preliminary exposure metrics and focus on constructing a simple classification scheme to categorize buildings and properties by a 5-level Likert-scale ranking: 1: very low, 2: low, 3: medium, 4: high, and 5: very high, flood risk, based on a cumulative exposure index for each element-at-risk derived from the integration of Table 2 features.

MODEL RESULTS

CoastFLOOD Model Validation

The CoastFLOOD model validation is performed with visual comparisons of simulation results against the US certified GIS map output of NOAA's SLR Viewer, provided by the Office for Coastal Management (https://coast.noaa.gov/digitalcoast/tools/slr.html). The CoastFLOOD model's performance was quantitatively evaluated by a Goodness-of-Fit, *GoF*, and a spatially averaged *Bias* metric of efficiency to reproduce the highest possible extent of Flooded Area (*FA*), and the largest achieved Floodwater Height (*FH*), respectively, on inland coastal plains:

$$GoF(FA) = \frac{FA_{mod} \cap FA_{NOAA}}{FA_{mod} \cup FA_{NOAA}} \quad , \quad Bias(FH) = \frac{\sum_{i=1}^{N} \left(\left| \frac{FH_{mod,i} - FH_{NOAA,i}}{FH_{NOAA,i}} \right| \right)}{N} \quad (5)$$

The simulated *FA* coincides with the NOAA SLR viewer GIS-app estimation when the two outputs exactly overlap against each other (*GoF*=1) whereas no agreement is hinted when no intersection of FAs occurs (*GoF*=0). The *i* index refers to the number of grid cells with *N* the maximum number of them.

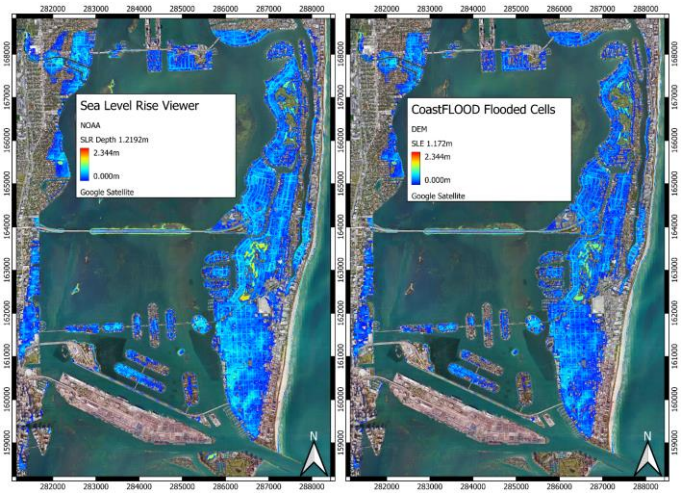

a **b**

Fig. 4. Comparisons of model results against output from NOAA SLR Viewer: a) map of flooded areas based on NOAA Viewer v.3.0.0 for SLR = 1.2 m (~4ft) along the coastline; b) map of flooded areas based on CoastFLOOD hydraulic simulations for SLE = 1.172 m along the coastline. Color maps refer to Floodwater Height (on NOAA's DEM).

CoastFLOOD model results (Fig. 4b) are compared against the estimations from NOAA SLR Viewer (Fig. 4a) under similar conditions of TWL (~1.2 m) responsible for coastal flooding. The impacted areas are almost identical for the two methods and the 2-D FH distribution is very similar. Namely, the *GoF(FA)* index scores quite high values >0.80, which increases drastically for even higher scenarios of TWL (e.g., ≥2 m) driving inundation in the study area (not shown for brevity). The relevant *Bias(FH)* falls under 10% everywhere

in the study region, scoring very low values in the most exposed areas. Note that the used land elevation data for the validation is based on NOAA's Digital Elevation Model (DEM), not DSM as in the following maps, in order to comply with NOAA SLR Viewer estimations. The use of a reduced complexity hydraulic flow model (e.g., CoastFLOOD in our case) may provide more realistic estimations (Fig. 4b) compared to the more simplistic Bathtub approach (Fig. 4a) that usually overestimates the extension of the flood.

Coastal Inundation Model Output

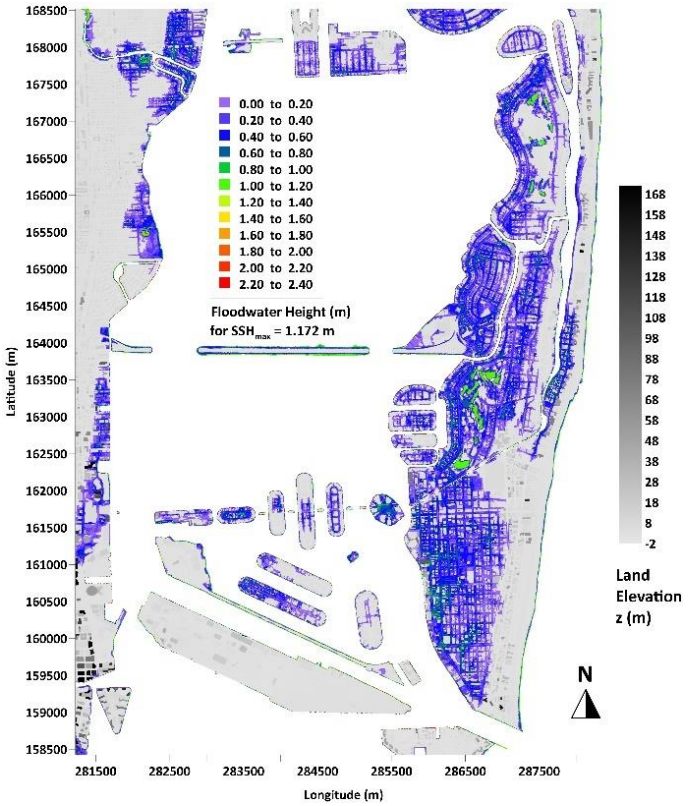

Fig. 5. Map of flooded areas portraying the Floodwater Height, FH (m), over the inundated study region of southcentral Miami based on simulations with CoastFLOOD model over the DSM domain for the Hurricane Irma scenario of the absolute TWL maximum during the 30-year period 1994-2023.

The *FH* (or flood depth) is the water level above ground at a specified location and it is the outcome of the momentum of storm tide seawater that elevates and accumulates on low-land areas. It practically determines how high the inundation water level can rise in open spaces and in the vicinity of a building or within a property area. According to FEMA (2018) storm surge flooding from Hurricane Irma ranged between 1.25 m (4.1 ft) and 2.44 m (8 ft) above ground in the downtown area of MDC, which corroborates the CoastFLOOD model results shown in Fig. 5. FH is selected as the leading parameter in assessing the exposure and vulnerability of a property, as it is a primary cause of damage to buildings during storm surge flooding (FEMA, 2018). According to the latter, buildings within or in touch with a FH ≥ 1 m are clearly within moderate to high flood risk zones, based on the projected amount of damage that they will sustain. Under such conditions, Chao et al. (2021) pinpoint the inability of first-level responder rescue teams to operate using terrestrial vehicles and on foot. Moreover, the high fatality risk by drowning, induced by *FH* > 2 m, as house ceilings may trap people in floodwater inside single-story buildings (Creach et al., 2015). Thus, the relatively low elevation of the MDC coastal study area with a mean *z* = 1.82 m (6 ft) above MSL suggests an increased exposure to storm surge.

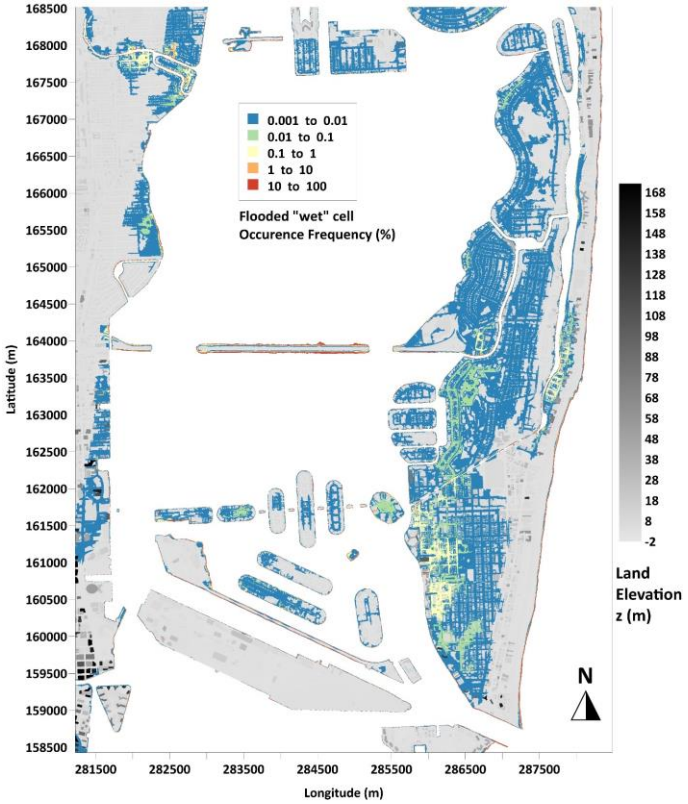

Fig. 6. Map of occurrence probabilities (%) for FAs (flooded "wet" cells) over the study region of southcentral Miami derived from simulated inundation extents due to daily sea level values during 1994-2023.

Our flood hazard analysis is further supported by the occurrence probabilities for flooded areas (i.e., defined as "wet" cells; Fig. 6) over the potentially inundated study region of southcentral Miami, based on simulations with CoastFLOOD model for daily data of maximum TWL during the entire 30-year period of 1994-2023. The coastal areas are more frequently impacted than the inland ones, while there are obvious clusters of low-land properties that suffer the by 1‰–1‰ up to 1% of the time, especially in the leeward side of southwestern Miami Beach and several areas on the more exposed island barriers and near the internal water channel network (green and yellow color areas). The evolution of the FCP_j (Androulidakis et al., 2023a) shows that extreme *FCPs* (>median+σ and >median+2σ) are more frequent after 2012 (Fig. 7a) in agreement with the respective TWL rise (Fig. 3b). A clear shift during the last decade compared to the previous period, is also derived from the FCP annual frequencies (μ2-μ1=8%). The highest *FCPs* (>median+σ) are characterized by a positive trend of 3.2%/decade over the 30-year period (Fig. 7b).

FLOOD IMPACT ASSESSMENT

Flood Impacts per Property over the Urban Study Area

To assess the local distributions of flood impacts on construction elements within the urban morphology, a property-level typology has been identified, considering how property features might affect their

resilience to coastal inundation. Fig. 8 presents maps of the "flood vicinity" metric (exposure feature A/A 8 in Table 2) as the distance of each discrete property from flood boundaries of inundated areas for one low- and one high-intensity scenario of TWL along the coastline. It is obvious that there are higher grounds far away from the coastline in the metropolitan area of MDC and the southcentral hillocks of Miami Beach, which are naturally protected for a medium/normal flood event (Fig. 8a). However, for high-impact events, such as Hurricane Irma flood, the potential impacted areas, vicinal to flood boundaries, increase (expanded area of impact in Fig. 8b vs. 8a).

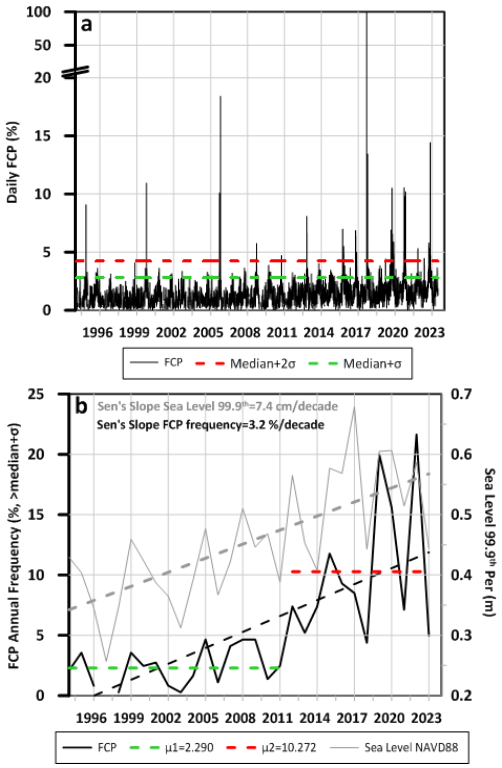

Fig. 7. (a) Daily evolution of Flood Coverage Percentage (FCP, %) during the 1994-2023 period and the respective thresholds of median+σ (green line) and median+2σ (red line). (b) Evolution of the annual occurrence frequencies (%) of FCP that exceed the median+σ threshold (black line) and the annual 99.9th SL percentiles. The μ1 (green line) and μ2 (red line) means derived by the Pettit homogeneity test, the linear trends and the Sen's Slopes are also marked.

Fig. 9. portrays a property-level flood map presenting the mean FH per discrete plot holding in the study region for Hurricane Irma condition of inundated areas (TWL = 1.172 m). The identified floodwater flow paths, depicted in Fig. 5, lead to the inundation depth patterns of Fig. 9 indicating neighborhoods highly susceptible to coastal flooding during hurricanes. Furthermore, the presence of properties in direct contact with the coastline at various parts of the western Biscayne Bay coastal stretch, the barrier islands' shores, and inside the canals of Miami Beach, highlights the potential for localized major flooding (red areas). Identifying these low-lying unprotected areas with a potentially substantial floodwater buildup is crucial for understanding the coastal flood risk and implementing measures to minimize inundation impacts. As such, the eastern part of Miami Beach along the Atlantic Ocean shores is protected by the grass-planted sand dune and the seaside promenade, which can mitigate the effects of rising sea levels at a large urban part behind them and along the beach (downstream flood route).

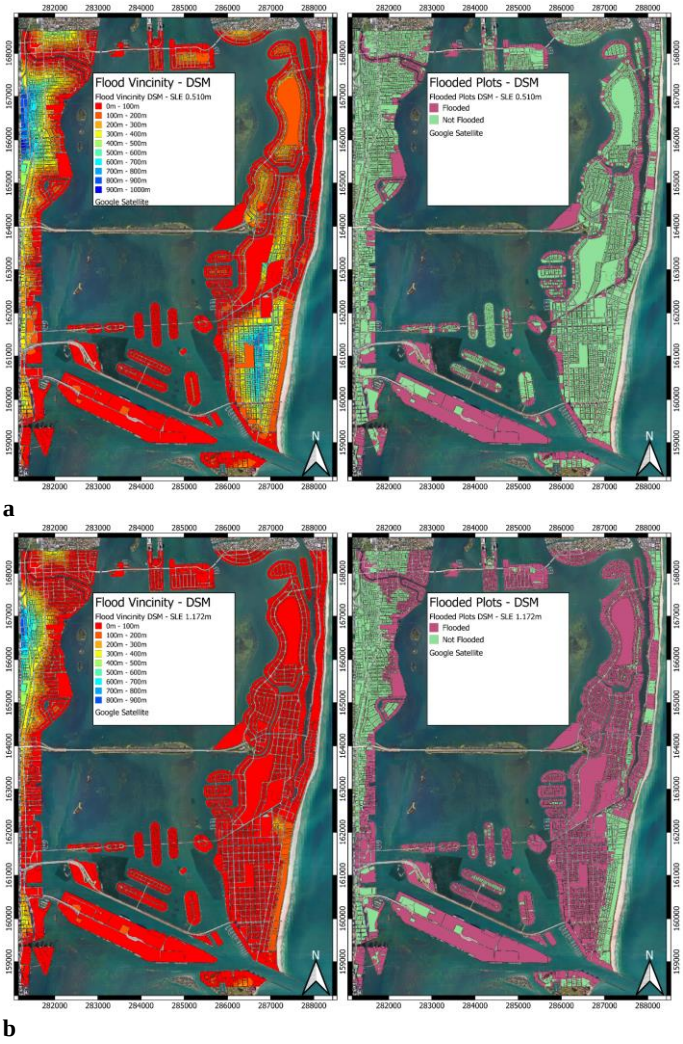

Fig. 8. Map of distance (exposure feature A/A 8 in Table 2) of each discrete property from flood boundaries of inundated areas (i.e., flood vicinity to plot holdings) based on DSM topography for (a) SLE=0.51 m (Scenario 5; Table 1) and (b) SLE=1.172 m (Scenario 1; Table 1) along the coastline. Left panels: distances per property plot; Right panels: binary map of flooded and non-inundated areas (30-year impacts).

Fig. 10 portrays the mean flood probability of impacted individual properties per each discrete plot holding area over the study region, based on simulations with CoastFLOOD model for daily data of maximum TWL on the coast during the 1994-2023 period. The port area demonstrates a significant propensity for floodwater pooling from the sea, but this is expected during severe weather conditions, since the terminal terrain is very smooth constructed of impermeable material (concrete/asphalt), with quite low elevation, and with no natural protection by plants and trees. Rather frequent (>1%) ponding might also be experienced by coastal residencies along the shores of the northeastern internal canal (Indian Creek), as well as several houses on the beaches of the barrier islands, yet with estimated flood depths rarely exceeding 50 cm. The identified potentially impacted areas by localized inundation effects could lead to property and building damages or loss inside (individual assets) and around a house (e.g., cars, bicycles, garden structures, etc.), as well as traffic disruption, port downtime, and operation recess of utility companies and infrastructures.

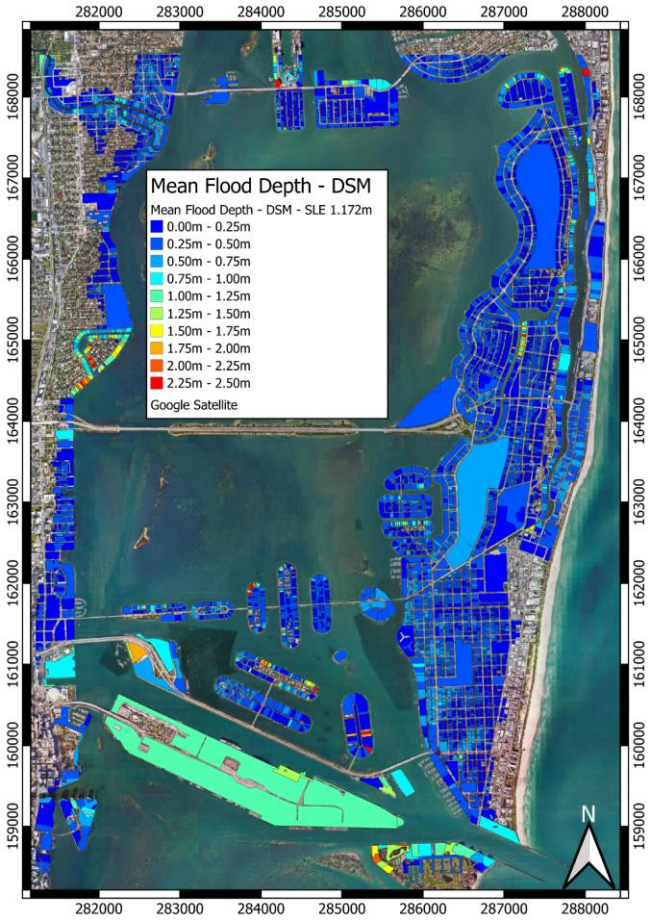

Fig. 9. Map of flooded properties portraying the average floodwater depth (m) per each discrete plot holding area over the inundated study region of southcentral Miami, based on simulations with CoastFLOOD model for Hurricane Irma (SLE = 1.172 m).

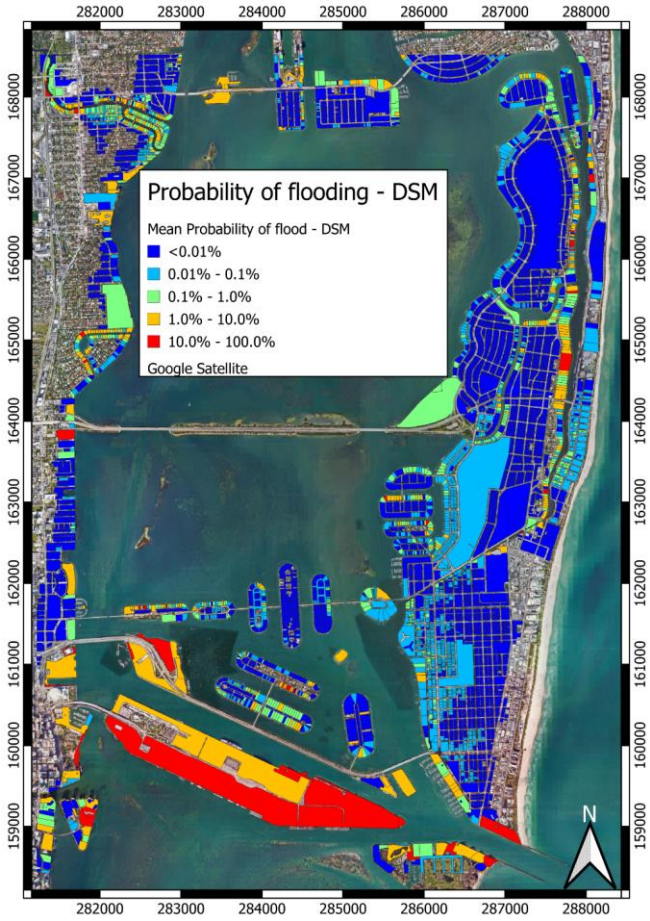

Fig. 10. Map of mean flood probability for impacted properties per each discrete plot holding area over the potentially inundated study region of southcentral Miami, based on simulations with CoastFLOOD model for daily data of sea level on the coast during the 1994-2023 period.

A combinatory analysis of the highly impacted areas of Figs. 9 and 10 can illustrate the resulting flood exposure of properties during storm events, setting the ground for the indication of high flood risk areas, after a future proper analysis of residential vulnerability and resilience to damage from flooding (e.g., investigating the number and elevation of floors, the type and quality of structure, the existence of protective elements, the foundation types, construction impermeability features, existence of individual flood barrier systems or water pumps), in order to prioritize adaptation and mitigation measures.

Fig. 11 completes the exposure analysis of potentially flooded properties by portraying the percentage of inundated area within each discrete plot holding over the study region. The diversification of impacted properties during an extreme event (Hurricane Irma) is immense, with adjacent plot holdings showing major and minor flood coverage, which indicates the need for further high-resolution assessment of the vulnerability to coastal floods at property-level.

CONCLUSIONS

This study combines the attributes of a robust hydraulic flood flow model for coastal inundation with a detailed assessment of property-level exposure to seawater floods in Miami-Dade County (FL, USA), focusing on the littorals of Biscayne Bay and Miami Beach. A preliminary extreme value analysis and statistical processing of recorded TWL timeseries is employed to build simulation scenarios.

The high-resolution model outputs can help to identify critical seawater flow paths and assess the numbers and characteristics of inundated properties via an all-inclusive exposure analysis per extreme storm tide scenario. CoastFLOOD model can provide valuable insight into the occurrence frequencies, the flooded area percentages, the floodwater heights in and around individual properties, highly susceptible to inundation. The estimated likelihood of coastal flood exposure to properties set the ground for a proper vulnerability assessment of urban features that can lead to a property-level flood risk management. This study aspires to facilitate a better understanding of the urban flood hydrodynamics in coastal areas of Miami. We introduce a tool to identify individual properties (and roads or open spaces) particularly susceptible to floodwater accumulation during severe storm surge events due to hurricanes, which can lead to particularly disastrous conditions in densely populated coastal cities. Thus, as a future goal, a simple classification scheme will be used to categorize buildings at a 5-level Likert-scale ranking by very low to very high flood risk, based on a cumulative exposure index derived from the presented exposure metrics herein, while also assessing the property-level vulnerability to coastal flooding. The results will be combined with a Hedonic regression model to use outputs in real-estate appraisal, and future projections of Consumer Price Index. Scenarios of new coastal protection projects will also be assessed.

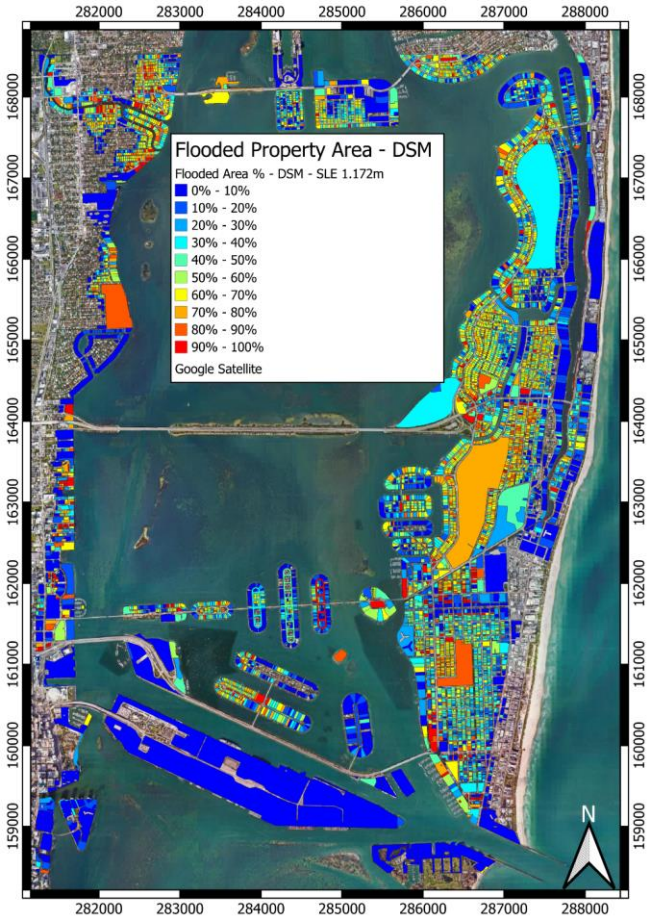

Fig. 11. Map of flooded properties portraying the percentage of inundated area within each discrete plot holding over the study region, based on CoastFLOOD simulations for Hurricane Irma (SLE = 1.172 m).

REFERENCES

Androulidakis, Y, Makris, C, Mallios, Z, and Krestenitis, Y (2023a). "Sea level variability and coastal inundation over the northeastern Mediterranean Sea," *Coast Eng J*, 65(4), 514-545.

Androulidakis, Y, Makris, C, Mallios, Z, Pytharoulis, I, Baltikas, V, and Krestenitis, Y (2023b). "Storm surges and coastal inundation during extreme events in the Mediterranean Sea: the IANOS Medicane," *Natural Hazards*, 117, 939-978.

Bates, PD, Horritt, MS, and Fewtrell, TJ (2010). "A Simple Inertial Formulation of the Shallow Water Equations for Efficient Two-Dimensional Flood Inundation Modelling," *Can J Fish Aquat Sci*, 387 (1–2): 33–45.

Chao, SR, Ghansah, B, and Grant, RJ (2021). "An exploratory model to characterize the vulnerability of coastal buildings to storm surge flooding in Miami-Dade County, Florida," *Appl Geogr*, 128, 102413.

Conte, MN, and Kelly, DL (2018). "An imperfect storm: Fat-tailed tropical cyclone damages, insurance, and climate policy," *J Environ Econ Manag*, 92, 677-706.

Creach, A, Pardo, S, Guillotreau, P, and Mercier, D (2015). "The use of a micro-scale index to identify potential death risk areas due to coastal flood surges: Lessons from storm Xynthia on the French Atlantic coast," *Nat Hazards*, 77(3), 1679–1710.

Darlington, C, Raikes, J, Henstra, D, Thistlethwaite, J, and Raven, EK (2024). "Mapping current and future flood exposure using a 5-metre flood model and climate change projections," *Nat Hazards Earth Syst Sci Discuss* [preprint].

Federal Emergency Management Agency (FEMA) (2018). *Mitigation assessment team report hurricane Irma in Florida. Building performance observations, recommendations and technical guidance*, FEMA P-202, December 2018.

Galiatsatou, P, Makris, C, Krestenitis, Y, and Prinos, P (2021). "Nonstationary Extreme Value Analysis of Nearshore Sea-State Parameters under the Effects of Climate Change: Application to the Greek Coastal Zone and Port Structures," *J Mar Sci Eng*, 9(8), 817.

Genovese, E, Hallegatte, S, and Dumas, P (2011). "Damage assessment from storm surge to coastal cities: Lessons from the Miami area," *Adv Geoinfo Sci Chang World*, 21-43.

Gilleland, E, and Katz, RW (2016). "extRemes 2.0: An Extreme Value Analysis Package in R," *J Statist Soft*, 72(8), 1–39.

Ghorbanzadeh, M, Vijayan, L, Yang, J, Ozguven, EE, Huang, W, and Ma, M (2021). "Integrating evacuation and storm surge modeling considering potential hurricane tracks: The case of hurricane Irma in Southeast Florida," *ISPRS Int J Geo-Info*, 10(10), 661.

Iliadis, C, Galiatsatou, P, Glenis, V, Prinos, P, and Kilsby, C (2023). "Urban Flood Modelling under Extreme Rainfall Conditions for Building-Level Flood Exposure Analysis," *Hydrol*, 10(8), 172.

Jones, MC, Wingard, GL, Stackhouse, B, Keller, K, et al. (2019). "Rapid inundation of southern Florida coastline despite low relative sea-level rise rates during the late-Holocene," *Nature Comm*, 10(1), 3231.

Katirtzidou, M, Skoulikaris, C, Makris, C, Baltikas, V, Latinopoulos, D, and Krestenitis, Y (2023). "Modeling stakeholders' perceptions in participatory multi-risk assessment on a deltaic environment under climate change conditions," *Env Mod Assess*, 28, 367–388.

Kourafalou, V, Androulidakis, I, Makris, C, and Mallios, Z (2024). "Climate impacts on the coastal environment of South Florida: Marine Heat Waves and Coastal Flooding," *AGU 2024 Ocean Sciences Meeting*. New Orleans, Louisiana, USA.

Makris, C, Androulidakis, Y, Mallios, Z, Baltikas, V, and Krestenitis, Y (2022). "Towards an Operational Forecast Model for Coastal Inundation due to Storm Surges: Application during Ianos Medicane," *Proc 9th Int Conf Civ Protect & New Tech*, Thessaloniki, SafeThessaloniki, 69-72.

Makris, C, Mallios, Z, Androulidakis, Y, and Krestenitis, Y (2023). "CoastFLOOD: A High-Resolution Model for the Simulation of Coastal Inundation Due to Storm Surges," *Hydrol*, 10(5), 103.

Neal, J, Villanueva, I, Wright, N, Willis, T, Fewtrell, T, and Bates P (2012). "How Much Physical Complexity is Needed to Model Flood Inundation?," *Hydrol Process* 26(15), 2264–2282.

Palm, R, and Bolsen, T (2020). *Climate change and sea level rise in South Florida*, Vol. 34, Springer International Publishing.

Paulik, R, Stephens, S, Wild, A, Wadhwa, S, and Bell, RG (2021). "Cumulative building exposure to extreme sea level flooding in coastal urban areas," *Inter J Dis Risk Reduct*, 66, 102612.

Pinelli, JP et al. (2018). "Overview of damage observed in regional construction during the passage of Hurricane Irma over the State of Florida," *8th Congr Forens Eng*, Reston, USA, 1028-1038.

Sun, H, Zhang, X, Ruan, X, Jiang, H, Shou, W (2024). "Mapping Compound Flooding Risks for Urban Resilience in Coastal Zones: A Comprehensive Methodological Review," *Remote Sens*, 16, 350.

Skoulikaris, C, Makris, C, Katirtzidou, M, Baltikas, V, and Krestenitis, Y (2021). "Assessing the vulnerability of a deltaic environment due to climate change impact on surface and coastal waters: the case of Nestos River (Greece)," *Env Mod Assess*, 26, 459-486.

Williams, SJ, and Gutierrez, BT (2009). "Sea-level rise and coastal change: Causes and implications for the future of coasts and low-lying regions," *Shore & Beach*, 77(4), 13.